

EXPERIMENTAL STUDY OF THE FLOW PAST A ROW OF REGULARLY SPACED TUBES – FOURIER AND WAVELET CHARACTERIZATION

C. R. Olinto

crolinto@yahoo.com.br

M. L. S. Indrusiak

sperbindrusiak@via-rs.net

S. V. Möller

svmoller@vortex.ufrgs.br

Programa de Pós-Graduação em Engenharia Mecânica – PROMEC

Universidade Federal do Rio Grande do Sul – UFRGS

Rua Sarmento Leite, 425

90050-170 Porto Alegre, RS, Brasil

Abstract. *The behaviour of turbulent flows past a row of tubes of equal diameter and regularly spaced was experimentally studied in a wind tunnel assembly using hot wire anemometry and a pressure transducer. Flows past a row of tubes are observed in many engineering fields, like energy and process industries and oil prospecting. In heat exchangers, the undisturbed incident flow is set by the first row of tubes, generating the flow structures that travel through the bank until the fully turbulence dominates. Traditional Fourier analysis and the more recent wavelet analysis were used to characterize the flow phenomena. This paper presents the characterization of the flow just next a row of tubes of pitch to diameter ratio of 1.26, considered in the literature as a transition geometry where the behaviour of the flow can be unstable.*

Keywords. *turbulent flows, Fourier analysis, wavelet analysis, row of tubes.*

1. Introduction

Tubes arranged inline perpendicular to the flow are a usual geometry, e.g. offshore structures and grids, and can be view also as a first approach for more complex arrangements like tube banks, encountered in many engineering applications, like energy and process industry. The flow, undisturbed prior to the first row tubes, is set by them and then travels through the bank. The experiments of this study were performed with the purpose of characterize the flow behind a single row of tubes in a high blockage ratio wind tunnel facility. Wall pressure measurements were made for each tube, along with velocity measurements behind the tubes and in the gap jet.

Flows impinging over a single tube are a classical first approach for study of fluid-structure iterations, as in Blevins (1990). Flows past two or more tubes, in line or in tandem are also of great interest. Alam et al. (2003) studied the flow past two in line tubes, showing the main vortex frequencies and pointing out the non-stationary, bi-stable behaviour of the wake. The bi-stable wake is characterized by a biased flow that switches from one side to the other at irregular intervals of time. Le Gal et al. (1996), observed a non-stationary behaviour of the flow past a row of tubes. Configurations with three and four in-line tubes were also studied (Guillaume and LaRue, 1999) and wakes named quasi-stable, spontaneous fluctuation and forced fluctuation were observed. Zdravkovich and Stonebanks (1988) studied the flow through a tube row with pitch to diameter ratio from 1.1 to 1.2, and found biased wakes forming cells downstream the tubes. Their conclusions were based mainly in the analysis of pressure coefficients around the tubes.

The flow past a row of tubes shows coupled wakes in phase opposition for pitch to diameter ratios greater than two, while for ratios lower than two, the jets between the tubes are deviated and the wakes merge to form cluster (Le Gal et al., 1996). Under some conditions the flow is unstable and presents two or more modes.

The quoted studies were performed with the tubes assembled in the wind tunnel facility in order to have a low blockage ratio. This is not a true configuration for tube bundles of heat exchangers. In the present research work the flow past a row of tubes with low pitch to diameter ratio was experimentally studied. The tubes were assembled perpendicular to the wind tunnel main axis filling up the test section, presenting a blockage ratio of 84%. This arrangement simulates the first row conditions of a heat exchanger tube bundle.

2. Background

Turbulence, considered as a random phenomenon, is characterized by its mean and standard deviation values, Fourier auto and cross spectra, as well as auto and cross-correlation functions. Spectral analysis and correlation methods are adequate to study permanent signals but not to deal with transitory processes at different scales. More recent is the use of wavelets, enabling the study of turbulent phenomena without the steady assumption, being a useful complementary tool to Fourier analysis.

2.1. Fourier analysis

The Fourier transform of a discrete time series enables the study of the bulk spectral behavior of the random phenomenon represented by the series.

The Fourier transform of a finite function $x(t)$, given as a discrete time series, and its inverse are defined as:

$$x(f) = \frac{1}{2\pi} \sum_0^T x(t) e^{-ift} \quad (1)$$

and

$$x(t) = \sum_{-\infty}^{\infty} x(f) e^{ift} \quad (2)$$

The Fourier spectrum gives the energy distribution of the signal in the frequency domain and is evaluated over the entire time interval:

$$P_{xx}(f) = |x(f)|^2 \quad (3)$$

In practice, in order to minimize the random error, was used the power spectral density function (PSD) which is the Fourier spectrum of the series smoothed over frequency intervals and over an ensemble of estimates (Bendat and Piersol, 1971).

2.2. Wavelet analysis

While the Fourier transform uses trigonometric functions as basis, the bases of wavelet transforms are functions named wavelets. A wavelet is a finite energy function, $\psi(t)$, with a zero average, which satisfies an admissibility condition:

$$C_{\psi} = \int_0^{\infty} \frac{|\Psi(f)|^2}{f} df < \infty \quad (4)$$

where $\Psi(f)$ is the Fourier transform of the wavelet.

The wavelet function is also called mother wavelet, because it generates an entire set of wavelet basis:

$$\psi_{a,b}(t) = \frac{1}{\sqrt{a}} \psi\left(\frac{t-b}{a}\right), \quad a, b \in \mathbb{R}, \quad a > 0 \quad (5)$$

The parameters a and b are respectively scale and position coefficients.

The continuous wavelet transform (CWT) of a function $x(t)$ and its inverse are given by:

$$Wx(a, b) = \int_t x(t) \psi_{a,b}(t) dt \quad (6)$$

and

$$x(t) = \frac{1}{C_{\psi}} \int_b \int_a Wx(a, b) \psi_{a,b}(t) \frac{da db}{a^2} \quad (7)$$

The respective wavelet spectrum is defined as:

$$P_{xx}(a, b) = |Wx(a, b)|^2 \quad (8)$$

While the Fourier spectrum, Equation (3), gives the energy for each frequency over the entire time domain, in the wavelet spectrum, Equation (8), the energy is related to each time and scale (or frequency). This characteristic of the wavelet transform allows the representation of the distribution of the energy of the transient signal over time and frequency domains.

According to Percival and Walden (2000), the discrete wavelet transform (DWT) is a judicious sub sampling of CWT, dealing with dyadic scales, and given by:

$$D(j, k) = \sum_t x(t) \psi_{j,k}(t) \quad (9)$$

and its inverse transform:

$$x(t) = \sum_j \sum_k D(j, k) \psi_{j,k}(t) \quad (10)$$

where the scale and position coefficients (j, k) are dyadic sub samples of (a, b).

The discrete wavelet spectrum is defined by:

$$P_{xx}(j, k) = |D(j, k)|^2 \quad (11)$$

The Fourier transform of a finite series gives only a finite number of coefficients, depending on the length of the time series, and therefore neglects the coefficients related to the higher frequencies. Anyway, these frequencies are already filtered at the acquisition process, to prevent aliasing. In the wavelet transform of a finite series, the length of the series also restricts the number of computable coefficients but, unlike the Fourier transform, the remaining coefficients are related to the lower frequencies, including the mean value of the signal, and cannot be disregarded. In practice, the DWT of a series with more than 2^J elements is computed for $1 \leq j \leq J$, being J a convenient arbitrary choice. The remaining part of the signal, containing the mean values for a scale J, is given by:

$$A(J, k) = \sum_t x(t) \phi_{J,k}(t) \quad (12)$$

where $\phi(t)$ is the scaling function associated to the wavelet function.

The inverse transform of a discrete time series with sampling frequency F_s is done by:

$$x(t) = \sum_k A(J, k) \phi_{J,k}(t) + \sum_{j \leq J} \sum_k D(j, k) \psi_{j,k}(t) \quad (13)$$

where the first term is the approximation of the signal at the scale J, which corresponds to the frequency interval $[0, F_s/2^{J+1}]$ and the inner summation of the second term are details of the signal at the scales j ($1 \leq j \leq J$), which corresponds to frequency intervals $[F_s/2^{j+1}, F_s/2^j]$

3. Experimental Technique

The test section, shown schematically in Fig.1 is a rectangular channel, with 146 mm height and a width of 195 mm. Air was the working fluid, driven by a centrifugal blower, passed by a settling chamber and a set of honeycombs and screens, before reaching the tube row with about 1 % turbulence intensity.

Before the tube row a Pitot tube, at a fixed position, was applied to measure the reference velocity for the experiments. The Reynolds number, calculated with the tube diameter (32.1 mm) and the entrance (reference) velocity is $Re = 17500$.

Velocity and velocity fluctuations were measured by means of a DANTEC *StreamLine* constant temperature hot-wire anemometer. Pressure was measured by an ENDEVCO piezo-resistive pressure transducer, mounted inside one of the tubes of the row (Goulart, 2004). Fig. 2a shows the tube row and Fig. 2b shows a scheme of the instrumented tube and of the mounting technique of the transducer. The tube with the pressure transducer could be rotated, so that measurements of pressure fluctuations at the tube wall were performed at several angular positions.

Previous analysis of the behaviour of the test section, by means of METRA accelerometers, and of the measurement technique, allowed identifying peaks in spectra due to resonance not related to the investigated phenomena. Data acquisition of pressure and velocity fluctuations were performed simultaneously by a Keithley DAS-58 A/D-converter board controlled by a personal computer, which was also used for the evaluation of the results.

The tube row was mounted with 5 cylinders having a 32.1 mm diameter with pitch to diameter ratio of 1.26. The tube length was 146 mm and they were in close contact with both upper and lower horizontal walls.

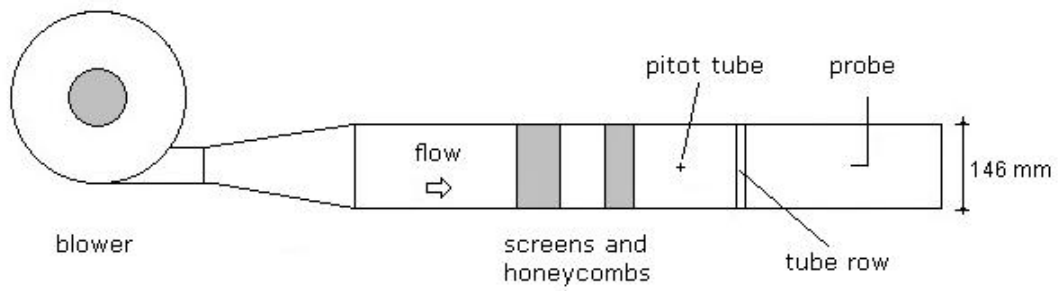


Figure 1. Test section

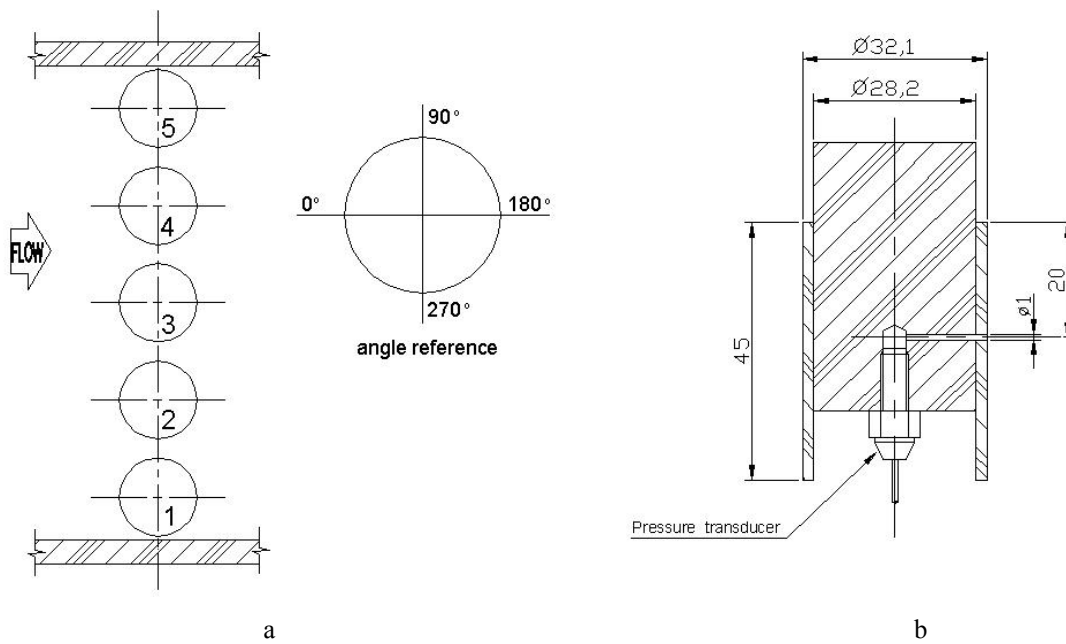


Figure 2. Mounting scheme a) tube row assembling; b) transducer support

4. Results

4.1. Pressure coefficient distribution and pressure fluctuation

Figure 3 shows pressure coefficient distribution ($CP = 2P/\rho U^2$) around the tubes and Fig. 4 shows pressure fluctuation around the tubes. The pressure coefficient distribution is very uniform and similar for all tubes, with de maximum at zero degree, and the negative pressure peak next 90° and 270°. These are the same points where maximum fluctuation occurs showing that they are also the shedding points. This is similar to the distribution observed in tube banks by Goulart et al. (2003) and differs from that of a single tube where the shedding points occur at 60-70° and 290-300° for the sub critical regime (Meneghini, 2002).

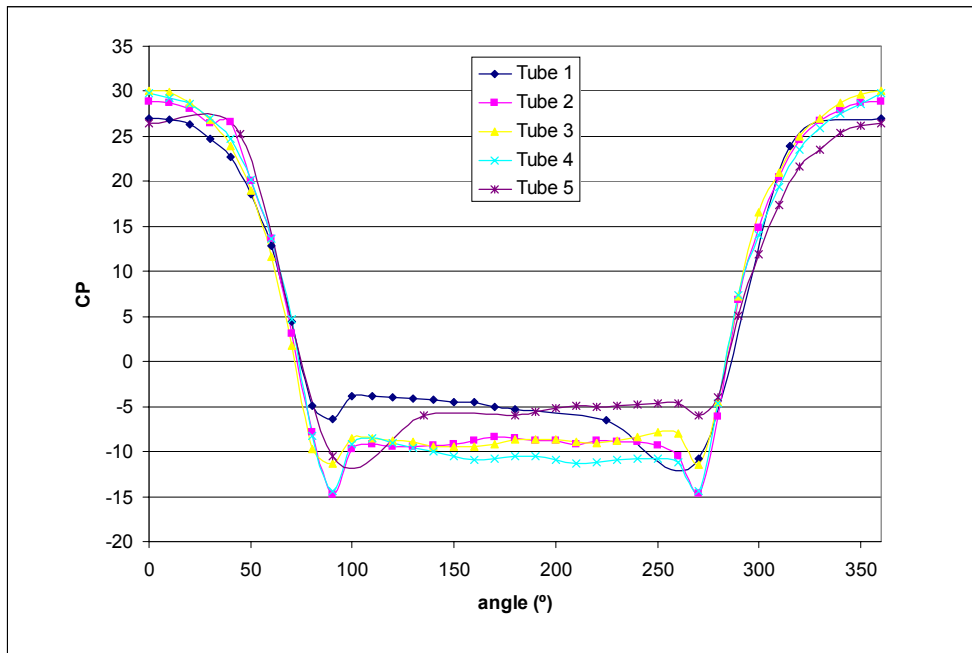


Figure 3. Pressure coefficient distribution.

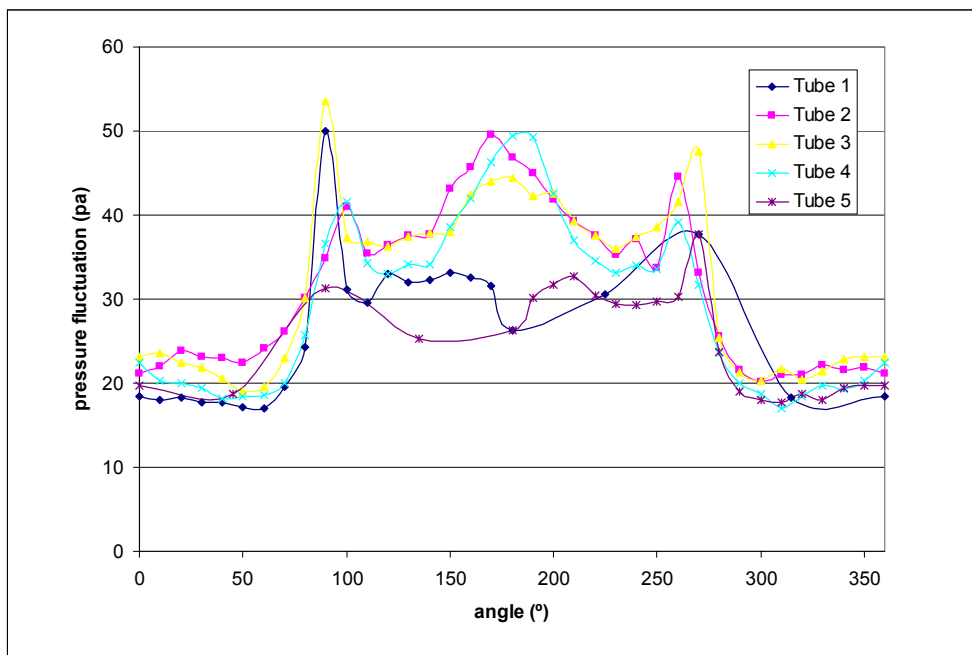


Figure 4. Pressure fluctuation

The symmetry of the pressure values at the narrow gap region and the similarity in the base pressure value (C_p at 180°) indicate that the jets arising from the gaps are not deviated, in contrast to what was found by Zdravkovich and Stonebank (1988) for an assembling with same gap width as in the present study, where biased wakes formed cells downstream the tubes. The present results can be explained by the fact that the relatively narrow tunnel and the small number of tubes could not deviate the flow due to fluid inertia.

4.2. Velocity analysis

For the analysis of velocity downstream the row of tubes, the series were acquired with a sampling frequency of 8 kHz and low pass filtered at 3 kHz.

In the near wake downstream the row not found narrow peaks in the spectrum, as can be shown in Fig. 5, indicating that there are not only one predominant shedding frequency, but just a relatively wide band of frequencies. The main

peaks in the spectra are at 180 Hz and they are as stronger as more distant from the row. The energy maximum occurs at a downstream distance from the centerline of the tube row, $x/d = 2.5$. This frequency corresponds to Strouhal number of 0.11, calculated based at gap velocity. This agrees with the frequencies presented by Blevins (1990) for similar tube array.

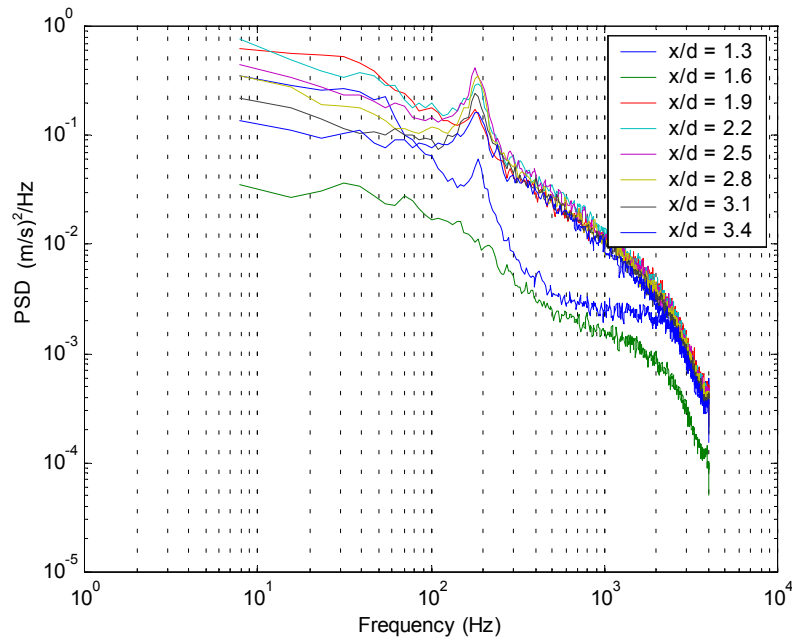


Figure 5. Power spectra (PSD), near wake velocity

Measurements made using X-probe in the wake of the center tube, 5 diameters downstream the row, show that the 180 Hz peak is still present and is more visible in the transversal velocity component (V_y). At 10 diameters downstream the row there are no more spectral peak at the velocity signal, indicating that the flow has a full developed turbulence characteristic (see Fig. 6).

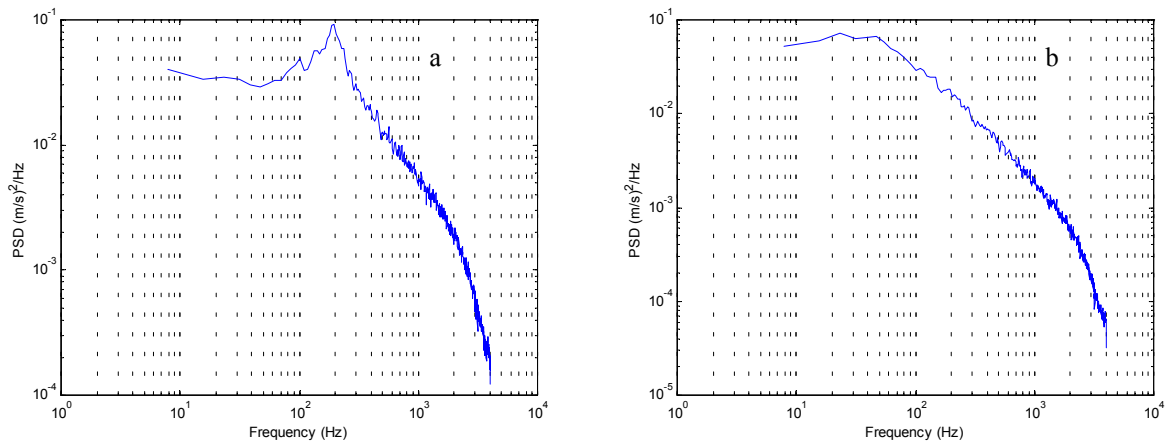


Figure 6. Transversal velocity power spectra: a) 5 d; b) 10 d

The continuous wavelet representation of the energy of two velocity signals measured at tangents to each tube of a single gap at position $x/d=2.5$ is shown in Fig. 7 and their respective Fourier spectra are in Fig. 8. While the Fourier spectra show that the energy of the wake is distributed over a relatively wider frequency interval than that of the wake of a single cylinder, at the wavelet spectra the temporal distribution of the energy of the wake is also visible, showing that the wake is not wide in frequency every time but instead wanders over the frequency interval along time, as in Fig. 7a, and can also presents intermittence, as in Fig. 7b.

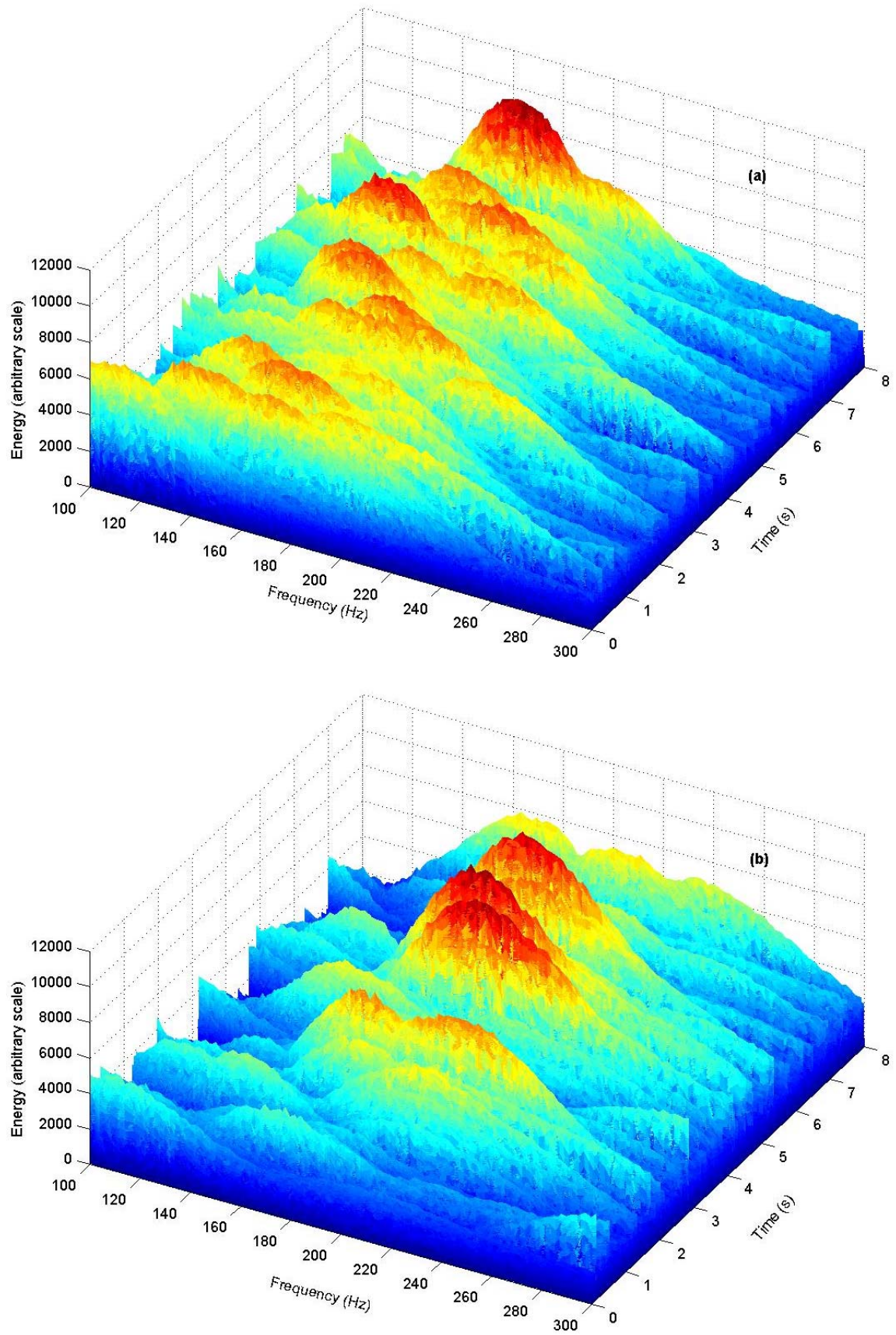


Figure 7: Continuous wavelet spectra of two velocity signals tangent to each tube of a single gap at position $x/d=2.5$. The respective power spectral density functions are in Fig. 8.

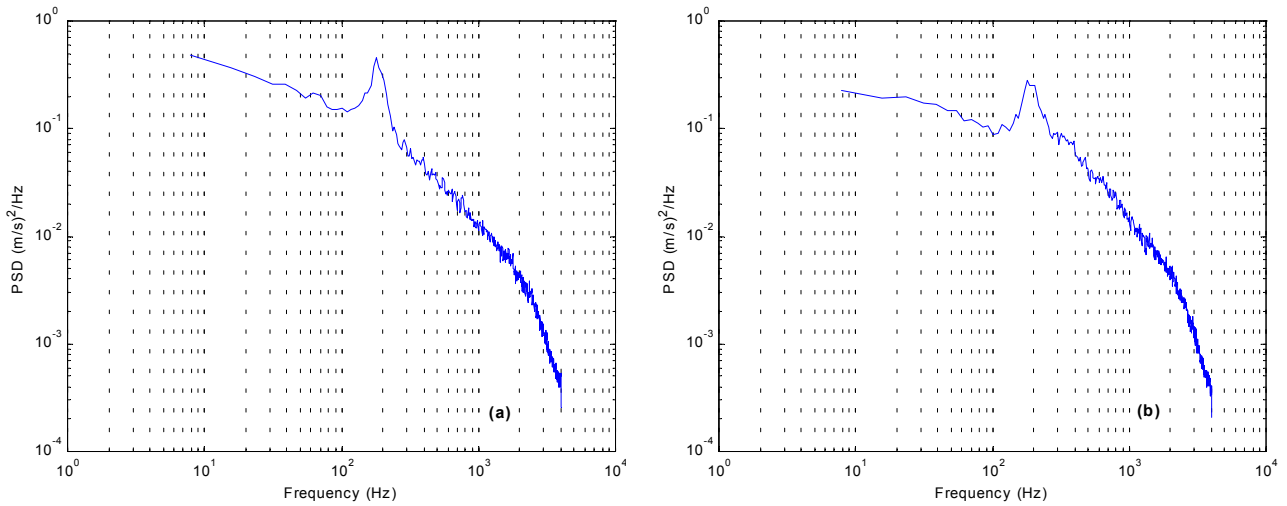


Figure 8: Power spectral density functions (Fourier) of the same signals as in Fig. 7.

Simultaneous measurements were made by placing two hot-wire probes in the tangents of each tube at the gaps between tubes 2 and 3, 3 and 4 and behind the central tube, at varying downstream distances from the centerline of the tube row (x/d). The cross correlations and a wavelet low pass filtered signal (0-4 Hz) were calculated and evidenced that inside the gaps there is a phase opposition flow near the gap. This characteristic decrease when the downstream distance increases (Fig. 8). Behind the central tube neither opposition phase nor phase flow were found, showing a more random characteristic (Fig.9).

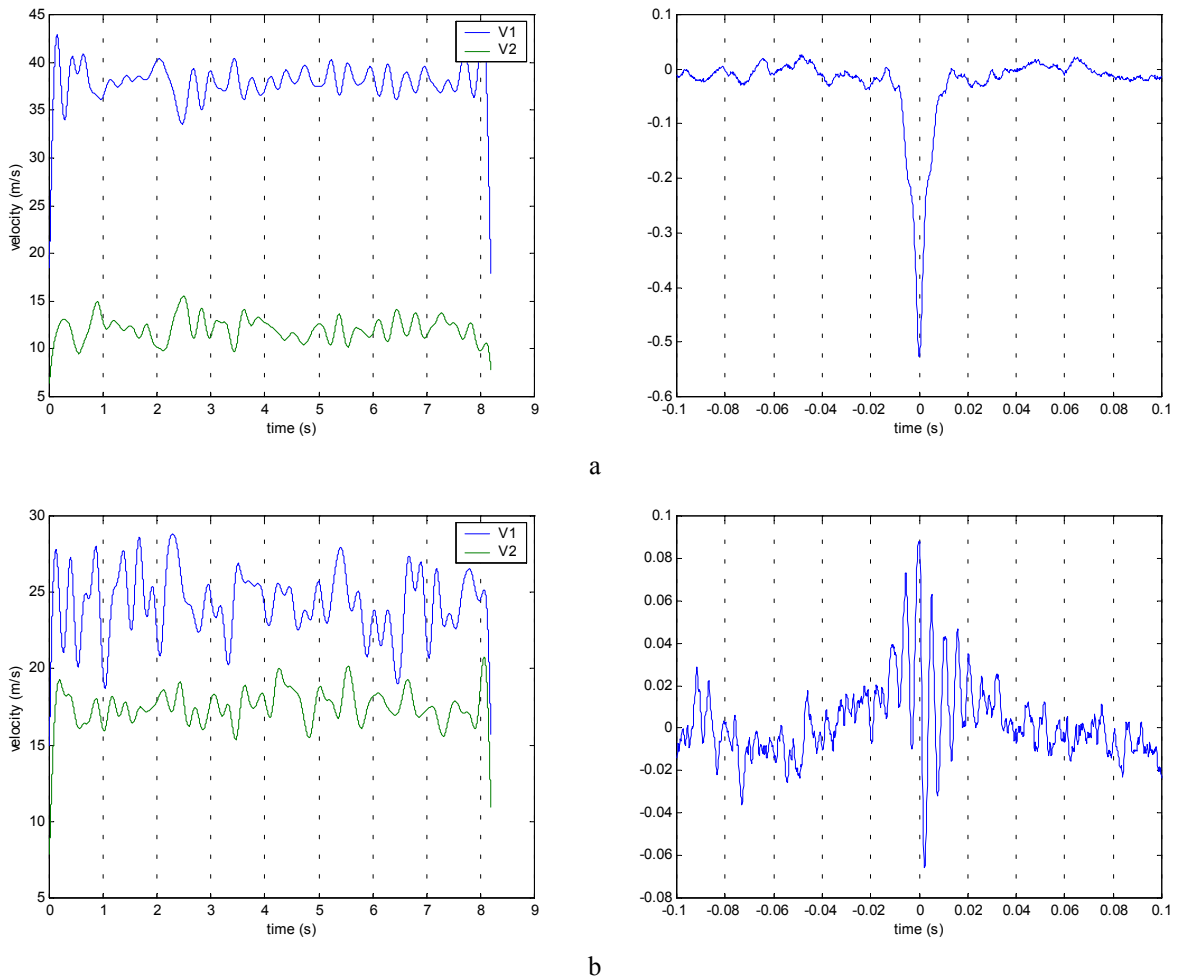


Figure 9. Wavelet approximation of the velocity signal corresponding to a frequency interval of 0 to 4 Hz and cross correlation of tangent velocity between tubes 3 to 4: a) $x/d = 1.25$; b) $x/d = 2.2$

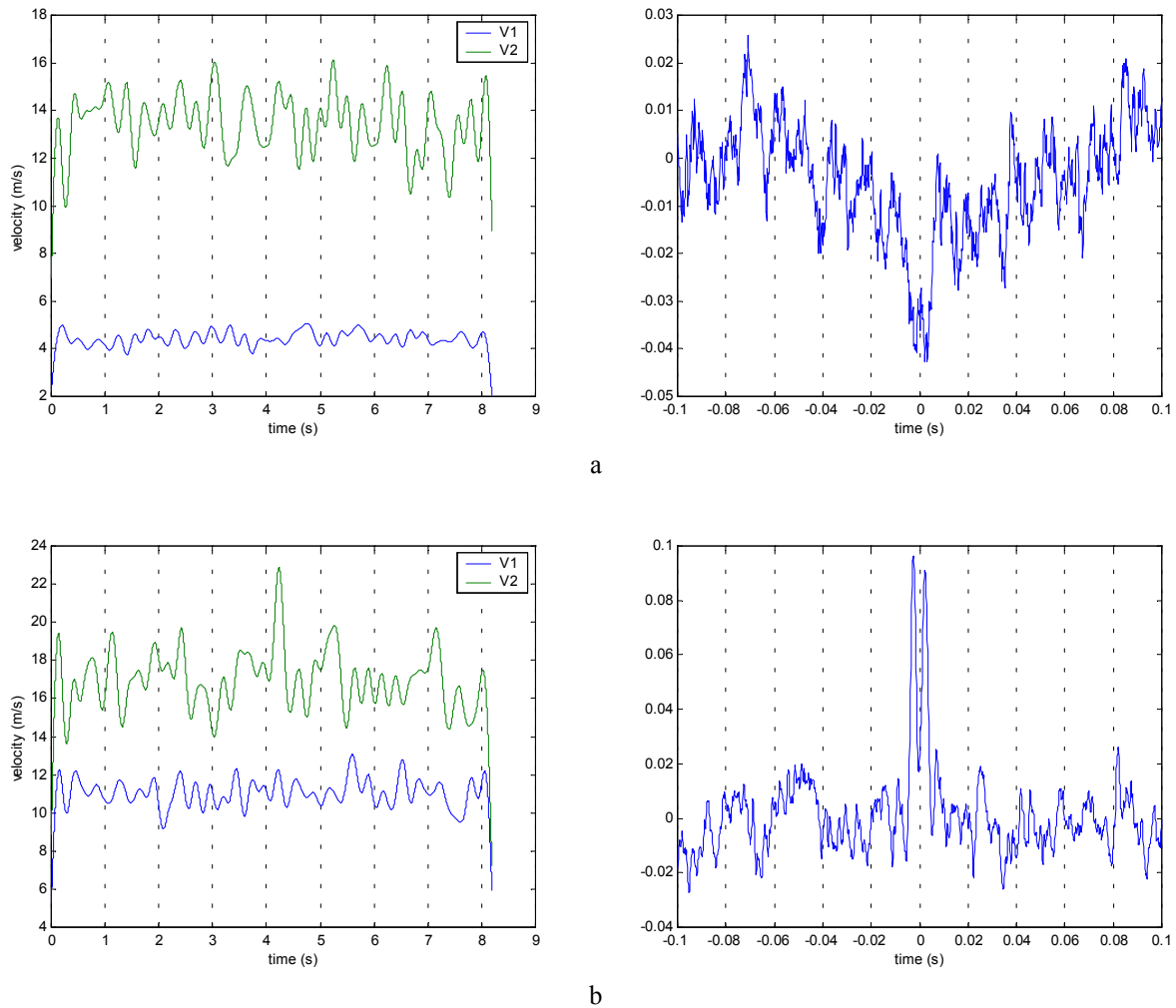


Figure 10. Wavelet approximation of the velocity signal corresponding to a frequency interval of 0 to 4 Hz and cross correlation of tangent velocity to the central tube a) $x/d = 1.25$; b) $x/d = 2.2$

5. Conclusions

This paper presents the experimental study of the velocity and wall pressure fluctuations in the turbulent flow downstream a tube row.

Only one shedding mode was observed, with no evidence of the presence of the bi-stable effect.

The pressure distribution around the tubes is very organized and symmetric; it presents just a deviation next the lateral wall on the outer tubes.

Velocity fluctuations measured simultaneously in the wake, with the probes aligned with the tube tangents, show that in the gap downstream region, next to the row, the fluctuations occur in phase opposition. The downstream velocity measurements with the probes aligned to the tangent of the central tube show no phase relation between this wake and those of the next gaps.

The spectra of velocity fluctuations show the principal peak appearing on the downstream intermediate distance (0,6 D to 2 D), at a frequency of 180 to 200 Hz corresponding to Strouhal numbers of 0,10 to 0,12, calculated with the gap velocity.

The phase opposition and in-phase flow were easily viewed when discrete wavelet transform was applied, acting as a low pass filter and thus, demonstrating the ability of wavelets as tools for analysing complex flow signals. The wavelet spectrum was also useful to enhance the knowledge about the wake, showing this behaviour along time.

6. Acknowledgements

Authors gratefully acknowledge the support by the CNPq - Brazilian Scientific and Technological Council, under the grants 414216/90-3, 400180/92-8 and 520986/1997-0.

Cláudio R. Olinto thanks CAPES, Ministry of Education, Brazil, also for granting him a fellowship (PICDT).

7. References

- Alam, Md. M., Moriya, M. e Sakamoto, H., 2003, "Aerodynamic characteristics of two side-by-side circular cylinders and application of wavelet analysis on the switching phenomenon", *Journal of Fluids and Structures* 18, pp. 325-346.
- Bendat, J. S. and Piersol, A. G., 1971, *Random Data: Analysis and Measurement Procedures*, Willey – Interscience, New York
- Blevins, R. D., 1990, "Flow-Induced vibrations", 2^a ed., Van Nostrand Reinhold, New York.
- Goulart, J. N., 2004, "Estudo experimental dos campos de pressão e velocidade em bancos de tubos com a utilização de defletores (Experimental study of pressure and velocity fields in tube banks with baffle plates)", Universidade Federal do Rio Grande do Sul.
- Goulart, J. N. V., Olinto, C. R. and Möller, S. V., 2003, "Experimental analysis of the turbulent flow inside a tube bank with baffle plates", in *Proceedings 17th Brazilian Congress of Mechanical Engineering*, São Paulo, Brazil.
- Guillaume, D. W., LaRue, J.C., 1999, "Investigation of the flopping regime with two-, three and four-cylinder arrays", *Experiments in Fluids* 27, pp. 145-156.
- Meneguini, J., 2002, "Mecânica da Geração e Desprendimento de Vórtices no escoamento ao Redor de Cilindros", *Anais da ETT 2002 - III Escola de Primavera de Transição e Turbulência*, pp. 217-344, Florianópolis, SC.
- Percival, D. B. e Walden, A. T., 2000, *Wavelet Methods for Time Series Analysis*, Cambridge University Press.
- Le Gal, P., Peschar, I., Chauve, M.P. e Takeda, Y., 1996, "Collective behaviour of wakes downstream a row of cilindres", *Phys. Fluids* 8, pp. 2097-2106.